eLIFE elifesciences.org

RESEARCH ADVANCE

A cell autonomous torsinA requirement for cholinergic neuron survival and motor control

Samuel S Pappas[1], Jay Li[1,2], Tessa M LeWitt[1], Jeong-Ki Kim[3,4,5], Umrao R Monani[3,4,5], William T Dauer[1,2,6]*

[1]Department of Neurology, University of Michigan, Ann Arbor, United States; [2]Cell and Molecular Biology Program, University of Michigan, Ann Arbor, United States; [3]Department of Cell Biology, Columbia University Medical Center, New York, United States; [4]Center for Motor Neuron Biology and Disease, Columbia University Medical Center, New York, United States; [5]Department of Pathology, Columbia University Medical Center, New York, United States; [6]Department of Cell and Developmental Biology, University of Michigan, Ann Arbor, United States

Abstract Cholinergic dysfunction is strongly implicated in dystonia pathophysiology. Previously (Pappas et al., 2015;4:e08352), we reported that Dlx5/6-Cre mediated forebrain deletion of the DYT1 dystonia protein torsinA (Dlx-CKO) causes abnormal twisting and selective degeneration of dorsal striatal cholinergic interneurons (ChI) (Pappas et al., 2015). A central question raised by that work is whether the ChI loss is cell autonomous or requires torsinA loss from neurons synaptically connected to ChIs. Here, we addressed this question by using ChAT-Cre mice to conditionally delete torsinA from cholinergic neurons ('ChAT-CKO'). ChAT-CKO mice phenocopy the Dlx-CKO phenotype of selective dorsal striatal ChI loss and identify an essential requirement for torsinA in brainstem and spinal cholinergic neurons. ChAT-CKO mice are tremulous, weak, and exhibit trunk twisting and postural abnormalities. These findings are the first to demonstrate a cell autonomous requirement for torsinA in specific populations of cholinergic neurons, strengthening the connection between torsinA, cholinergic dysfunction and dystonia pathophysiology.
DOI: https://doi.org/10.7554/eLife.36691.001

***For correspondence:** dauer@med.umich.edu

Competing interests: The authors declare that no competing interests exist.

Funding: See page 11

Received: 15 March 2018
Accepted: 16 August 2018
Published: 17 August 2018

Reviewing editor: Louis J Ptáček, University of California, San Francisco, United States

Introduction

Multiple lines of evidence implicate striatal cholinergic dysfunction in dystonia pathophysiology (***Pappas et al., 2015***; ***Albin et al., 2003***; ***Eskow Jaunarajs et al., 2015***; ***Pappas et al., 2014***). The symptoms of DYT1 dystonia, caused by a loss of function mutation in the gene encoding torsinA (***Ozelius et al., 1997***), are reduced by antimuscarinic treatments (*e.g.*, trihexyphenidyl)(***Burke et al., 1986***). Antimuscarinic agents also reduce motor (***Pappas et al., 2015***) and electrophysiological (***Maltese et al., 2014***) abnormalities in DYT1 mouse models. Striatal cholinergic dysfunction is a common feature of multiple DYT1 animal models (***Pappas et al., 2015***; ***Martella et al., 2009***; ***Pisani et al., 2006***; ***Sciamanna et al., 2012a***; ***Sciamanna et al., 2012b***), and experimental ablation of striatal cholinergic interneurons (ChI) can lead to abnormal postures (***Kaneko et al., 2000***).

We demonstrated previously that deletion of torsinA from forebrain GABAergic and cholinergic neurons (using Dlx5/6-cre; 'Dlx-CKO') causes highly selective degeneration of dorsal striatal ChI roughly coincident with the juvenile onset of abnormal limb clasping and twisting movements (***Pappas et al., 2015***). Selective ChI abnormalities are also present in postmortem tissue from DYT1 subjects (***Pappas et al., 2015***). Abnormal movements in Dlx-CKO mice are reduced by clinically relevant antimuscarinic treatments, strengthening model therapeutic validity and suggesting shared

pathophysiology with human dystonia. This work highlights the importance of elucidating the mechanism of selective ChI loss. A critical first step toward this goal is to determine whether the ChI loss observed in Dlx-CKO mice results from a cell autonomous role of torsinA in these cells or, alternatively, whether loss of torsinA from synaptically connected cells is also required. The major aim of these studies was to address this fundamental question.

To determine whether torsinA-related ChI loss is cell autonomous, we generated and characterized cholinergic neuron selective conditional torsinA knockout mice (ChAT-CKO). We find that ChAT-CKO mice phenocopy the selective degeneration of dorsal striatal ChI observed in Dlx-CKO mice (basal forebrain neuron numbers are normal in both models). Assessment of non-forebrain cholinergic populations demonstrates that pedunculopontine and laterodorsal tegmental brainstem cholinergic neurons, and spinal motor neurons also require torsinA for survival or normal function. ChAT-CKO mice exhibit severe motor and postural abnormalities that are distinct from Dlx-CKO mice. These findings are the first to establish a cell autonomous requirement for torsinA in ChI, as well as identifying additional vulnerable cholinergic neuron populations. This *in vivo* study fundamentally advances and expands understanding of the requirement of torsinA for normal cholinergic system function, opening new directions for the study of mechanisms contributing to selective neuronal dysfunction in dystonia.

Results and discussion

To determine if ChI neurodegeneration is a cell autonomous effect of torsinA loss, we conditionally deleted torsinA from cholinergic neurons (*Chat-IRES-Cre*$^{+}$, *Tor1a*$^{Flx/-}$; 'ChAT-CKO' mice; Cre-recombinase expression occurs before birth and is completely selective for cholinergic neurons; ***Figure 1—figure supplement 1*** [***Madisen et al., 2010***]). Unilateral unbiased stereology of ChAT-immunoreactive neurons in the dorsal striatum from 1 year old mice demonstrates a ~ 34% reduction in the number of dorsal striatal ChI in ChAT-CKO mice compared to control mice (***Figure 1A,B***). This finding was confirmed in an independent cohort using bilateral unbiased stereology (48% reduction; ***Figure 1—figure supplement 2A***). The number of striatal non-cholinergic neurons was not different from controls (***Figure 1—figure supplement 2B,C***), demonstrating that there are no secondary cell loss effects of ChI degeneration, and that torsinA loss of function-mediated neurodegeneration is highly specific. These findings establish a cell autonomous torsinA requirement for ChI survival.

ChI cell loss is strikingly selective in Dlx-CKO mice, occurring primarily in the dorsal aspects of the striatum, with approximately six times greater cell loss in the dorsolateral compared to ventromedial striatum (57% vs 9% cell density reduction in Dlx-CKO mice; [***Pappas et al., 2015***]). To examine if the cell autonomous ChI degeneration in ChAT-CKO mice follows a similar subregion-selective pattern, we determined the density of ChAT-immunoreactive neurons in each quadrant of the dorsal striatum (as previously [***Pappas et al., 2015***]). Significant reductions in ChI number were limited to the dorsolateral and dorsomedial segments of the dorsal striatum (72% and 54% cell density reductions in dorsolateral and dorsomedial, vs 12% and −4% in ventrolateral and ventromedial segments; ***Figure 1C***). This topographic pattern of cell loss was present throughout the entire rostro-caudal extent of the striatum (***Figure 1C,D***, ***Figure 1—figure supplement 3***). The dorsolateral selectivity of ChI neuron loss is highly relevant, as the dorsolateral striatum is a key motor circuit node functionally integrated according to topographic inputs, whereas ventromedial striatal neurons are connected in associative and limbic circuits (***Alexander et al., 1986***; ***Haber, 2016***; ***Parent and Hazrati, 1995***). In contrast, the basal forebrain contains cholinergic projection neurons subserving cognitive and attentional control (***Hasselmo and Sarter, 2011***; ***Ballinger et al., 2016***), which do not degenerate in either model (***Figure 1E,F***). Conditional deletion of torsinA from forebrain cholinergic neurons therefore mimics the region-selective vulnerability observed in Dlx-CKO mice, demonstrating a cell autonomous requirement for torsinA in select cholinergic populations. To determine if differing time courses of torsinA loss (via differing torsinA half lives) contributes to selective vulnerability, we assessed torsinA levels in dorsal vs ventral striatal ChI at P0. Surprisingly, despite uniform prenatal Cre recombinase expression and preferential loss of dorsal ChI, torsinA levels were reduced to a greater extent in ventral ChI (dorsal ChI contained 82% of control torsinA levels, while ventral ChI had ~52% remaining; ***Figure 1—figure supplement 4***). Non-vulnerable basal forebrain cholinergic

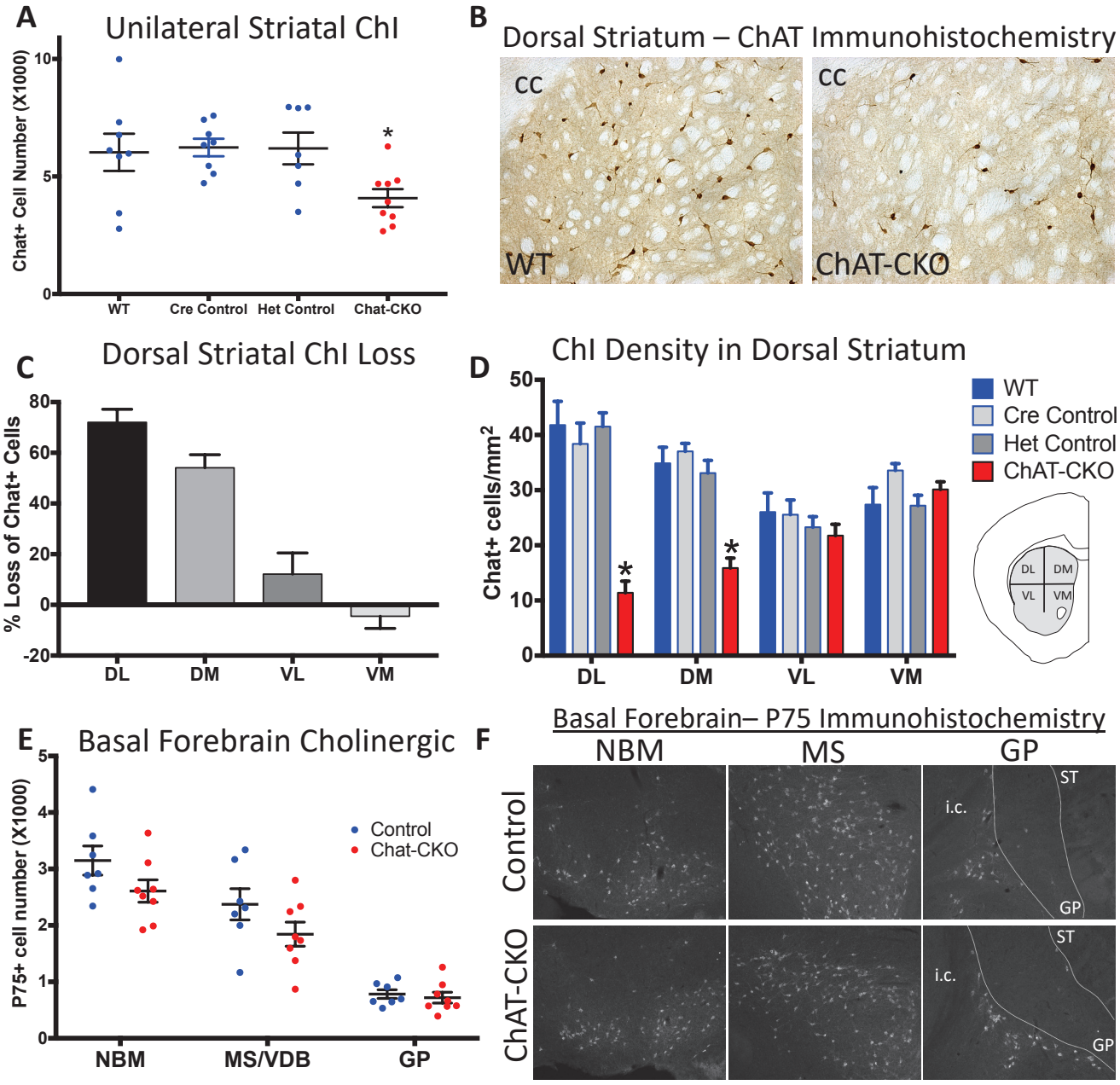

Figure 1. Conditional cholinergic neuron deletion of torsinA causes cell autonomous loss of striatal cholinergic neurons. (**A**) Unilateral stereological quantification of the number of ChAT-positive neurons in the striatum of ChAT-CKO and control mice (One-way ANOVA $F_{(3,28)} = 3.589$, p=0.02, Dunnett's multiple comparisons test: adjusted p value = 0.049; 'WT'=*Tor1a*$^{Flx/+}$; 'Cre Control'=ChAT-Cre+, *Tor1a* $^{Flx/+}$; 'Het Control'=*Tor1 a*$^{Flx/-}$; 'ChAT-CKO'=ChAT-Cre+, *Tor1a*$^{Flx/-}$). (**B**) ChAT immunohistochemistry of coronal sections containing dorsal striatum from WT and ChAT-CKO mice (cc = corpus callosum). (**C**) Percent reduction in cell density by striatal quadrant (DL = dorsolateral; DM = dorsomedial, VL = ventrolateral, VM = ventromedial). (**D**) Significant ChI loss is selective for dorsal striatal quadrants. Cell density quantification in control and ChAT-CKO striatal quadrants (Two-way ANOVA main effect of genotype $F_{(3,112)} = 24.02$, p<0.0001; main effect of quadrant $F_{(3,112)}=8.398$, p<0.0001; interaction $F_{(9,112)}=8.11$, p<0.0001. Post-hoc Tukey's multiple comparisons test). (**E**) Basal forebrain neurons are spared in ChAT-CKO mice. Stereological quantification of P75-immunoreactive basal forebrain cholinergic neurons in the nucleus basalis of meynert (NBM), medial septum/nucleus of the vertical limb of the diagonal band (MS/VDB), and globus pallidus (GP). No differences in the number of cholinergic neurons was observed (NBM,

Figure 1 continued on next page

Figure 1 continued

$t_{(13)}$=1.684, p=0.11; MS/VDB, $t_{(13)}$=1.537, p=0.148; GP, $t_{(13)}$=0.5, p=0.625). (**F**) P75 immunohistochemistry of sagittal sections containing basal forebrain cholinergic neuron populations. i.c. = internal capsule, ST = striatum.

DOI: https://doi.org/10.7554/eLife.36691.002

The following figure supplements are available for figure 1:

Figure supplement 1. ChAT-Cre is expressed prenatally.

DOI: https://doi.org/10.7554/eLife.36691.003

Figure supplement 2. Independent cohort confirmation of selective striatal cholinergic neuron loss in ChAT-CKO mice.

DOI: https://doi.org/10.7554/eLife.36691.004

Figure supplement 3. ChAT-positive neurons are reduced in a topographic pattern throughout the rostrocaudal extent of the dorsal striatum.

DOI: https://doi.org/10.7554/eLife.36691.005

Figure supplement 4. Time course of torsinA protein loss in dorsal and ventral striatum.

DOI: https://doi.org/10.7554/eLife.36691.006

Figure supplement 5. Time course of torsinA protein loss in basal forebrain.

DOI: https://doi.org/10.7554/eLife.36691.007

neurons exhibited 49% of control torsinA immunoreactivity (***Figure 1—figure supplement 5***). These findings demonstrate that a more rapid loss of torsinA during development does not contribute to the unique vulnerability of dorsal ChI.

TorsinA deletion is restricted to forebrain structures in Dlx-CKO mice. In contrast, ChAT-CKO mice lack torsinA in all cholinergic neurons throughout the neuraxis, enabling us to assess the impact of torsinA loss in additional cholinergic populations. Unbiased stereology of ChAT-immunoreactive neurons in the brainstem demonstrates significantly fewer cholinergic neurons in the pedunculopontine (PPN) and laterodorsal tegmental (LDT) nuclei in 1 year old Chat-CKO mice (***Figure 2A–D***). The PPN and LDT also contain GABAergic, and glutamatergic neurons (***Mena-Segovia, 2016***), which significantly outnumber cholinergic neurons (***Mena-Segovia et al., 2009***; ***Wang and Morales, 2009***). Unbiased stereology of NeuN +neurons in PPN and LDT showed no significant change in the overall number of neurons (***Figure 2A,C***). Because cholinergic neurons are a minority of cells in the PPN and LDT, it is possible that a significant reduction of this small sub-population cannot be detected when assessed by counting overall NeuN +neuron number. It is also possible that PPN and LDT cholinergic neurons exhibit reduced ChAT expression rather than actual cell loss. Regardless, either possibility demonstrates a cell autonomous role for torsinA for normal function of these cells. These findings also indicate that the loss or dysfunction of brainstem cholinergic neurons does not have deleterious effects on the viability of surrounding neurons. Consistent with this finding, there was no evidence of reactive microgliosis or astrogliosis in the brainstem (***Figure 2—figure supplement 1***). Quantification of the number of spinal motor neurons (C3-C5; [***Kim et al., 2017***]) demonstrated significantly fewer motor neurons in ChAT-CKO mice (***Figure 2E,F***).

The identification of cholinergic dysfunction or loss in PPN and LDT is notable, as considerable data implicate these cells in motor and postural control. PPN and LDT cholinergic neurons are distributed in a rostrocaudal continuum in the brainstem, forming a coordinated functional unit (***Mena-Segovia, 2016***; ***Mena-Segovia and Bolam, 2017***). PPN and LDT cholinergic neurons topographically innervate the striatum and striatal-projecting thalamic and midbrain dopamine neurons (***Dautan et al., 2014***), such that rostral PPN modulates motor-related circuits, LDT innervates limbic circuits, and caudal PPN targets both regions (***Mena-Segovia, 2016***; ***Xiao et al., 2016***) via both direct and indirect inputs. Consistent with a central role in modulating locomotor activity, optogenetic stimulation of PPN cholinergic neurons alters locomotion speed, while stimulation of adjacent glutamatergic neurons induces locomotion (***Xiao et al., 2016***; ***Roseberry et al., 2016***; ***Capelli et al., 2017***). Cholinergic PPN lesion alone or in combination with dopaminergic denervation impairs gait and causes postural abnormalities in primates (***Grabli et al., 2013***; ***Karachi et al., 2010***). In rodents, cholinergic-selective PPN lesion impairs performance on the accelerating rotarod and alters sensorimotor gating (***MacLaren et al., 2014a***; ***MacLaren et al., 2014b***), while non-specific PPN ablation alters gait (***Blanco-Lezcano et al., 2017***) and impairs reversal learning (***Syed et al., 2016***). Human neuroimaging and postmortem studies also provide support for a connection between PPN cholinergic integrity and motor function. PPN cholinergic loss is linked to gait abnormalities in Parkinson disease (***Karachi et al., 2010***; ***Bohnen et al., 2009***), and brainstem lesions (including PPN loss) can

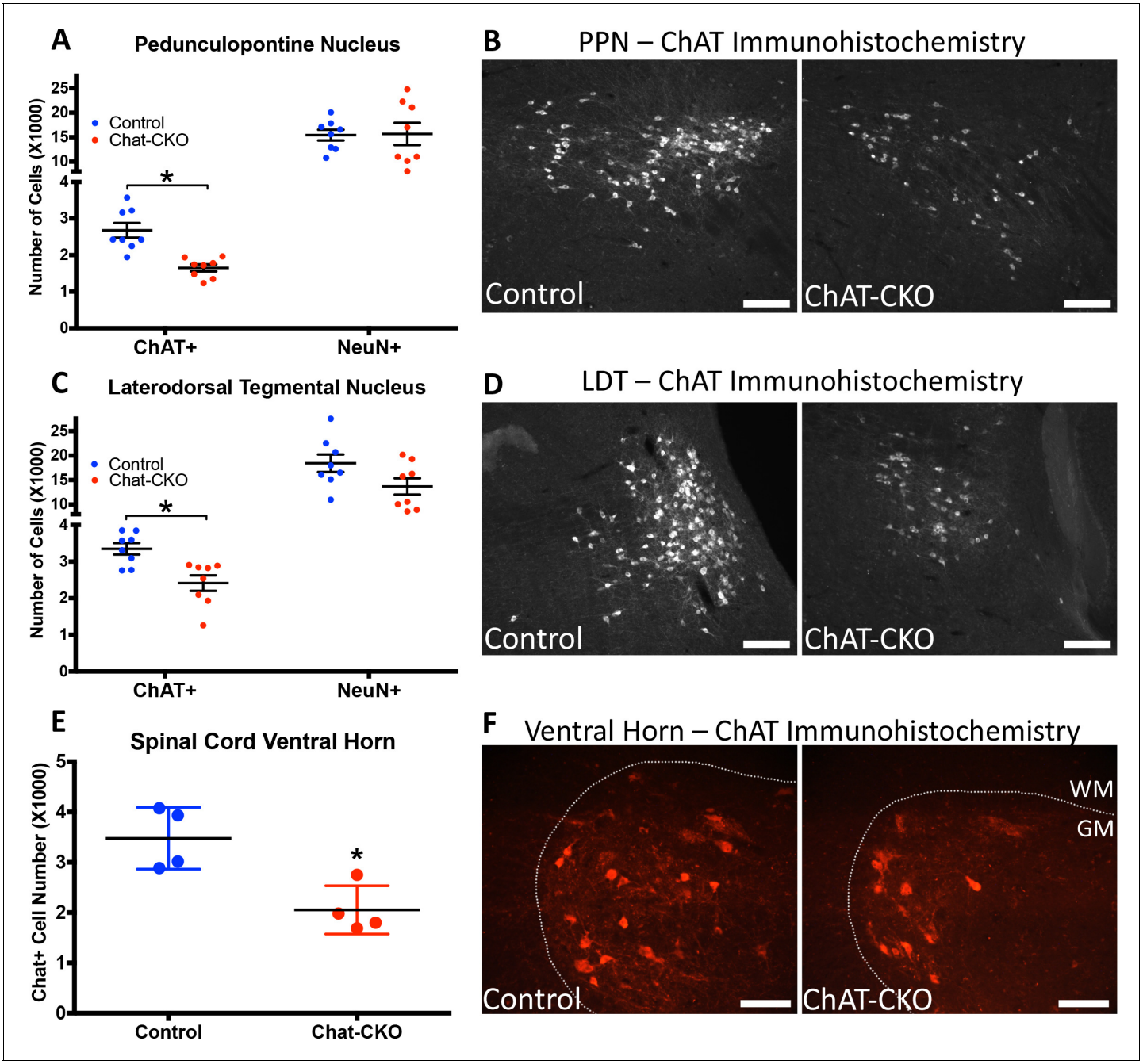

Figure 2. ChAT-CKO mice have significantly fewer brainstem and spinal cord cholinergic neurons. (**A,B**) Stereological quantification of ChAT-positive or NeuN-positive neurons in the pedunculopontine nucleus (PPN) of control and ChAT-CKO mice (ChAT; $t_{(14)}$=4.531, p=0.0005. NeuN; $t_{(14)}$=0.095, p=0.92). (**C,D**) Stereological quantification of ChAT-positive or NeuN-positive neurons in the laterdorsal tegmental nucleus (LDT) of control and ChAT-CKO mice (ChAT; $t_{(14)}$=3.571, p=0.003. NeuN; $t_{(14)}$=1.934, p=0.073). (**E,F**) Quantification of the number of ChAT-positive neurons in the cervical spinal cord of control and ChAT-CKO mice ($t_{(6)}$=3.654, p=0.0107). Scale bars = 100 μm.

DOI: https://doi.org/10.7554/eLife.36691.008

The following figure supplement is available for figure 2:

Figure supplement 1. Absence of gliosis in the brainstem of ChAT-CKO mice.

DOI: https://doi.org/10.7554/eLife.36691.009

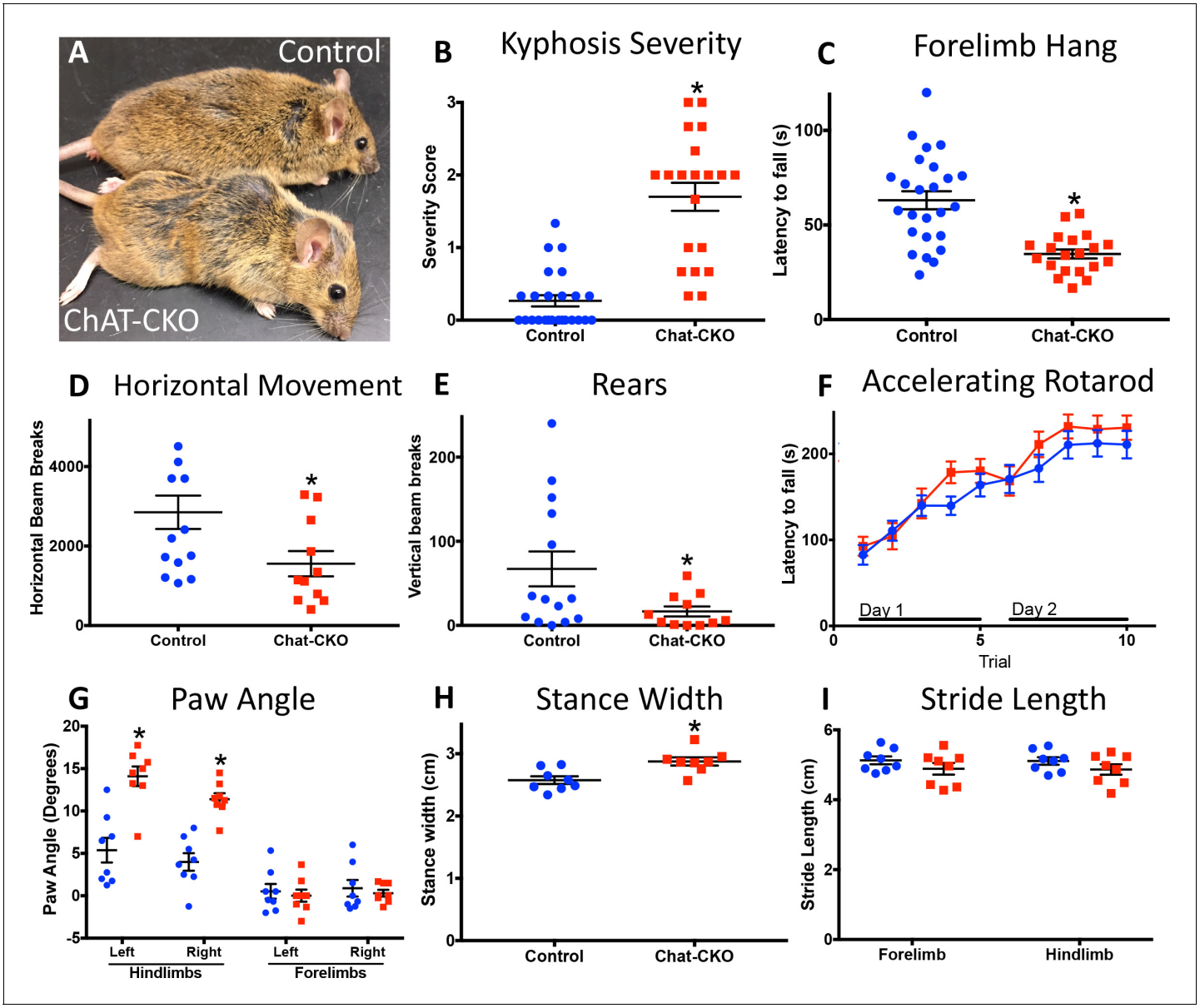

Figure 3. Motor behavior is severely disrupted in ChAT-CKO mice. (**A**) Representative image of a control and ChAT-CKO mouse demonstrates severe kyphosis and unkempt coat. (**B**) ChAT-CKO mice exhibit significantly increased kyphotic curvature during locomotion (Mann-Whitney U = 35, p<0.0001). (**C**) ChAT-CKO mice exhibit a significantly reduced latency to fall during forelimb suspension (Mann-Whitney U = 71.5, p<0.0001). (**D, E**) ChAT-CKO mice are hypoactive in the open field (horizontal movement, $t_{(23)}$=2.345, p=0.028; vertical rears, welch-corrected $t_{(15.1)}$ = 2.345, p=0.033). (**F**) Performance on the accelerated rotarod does not significantly differ from controls (two-way repeated measures ANOVA, genotype, $F_{(1,43)}$=0.75, p=0.389; trial, $F_{(9,387)}$=55.63, p<0.0001; interaction, $F_{(9,387)}$=1.194, p=0.297). (G - I) ChAT-CKO mouse gait is abnormal during locomotion (*paw angle*, two-way ANOVA main effect of genotype, $F_{(1,56)}$=30.54, p<0.0001, main effect of limb $F_{(3,56)}$=51.02, p<0.0001, interaction $F_{(3,56)}$=13.51, p<0.0001, post-hoc Sidak's multiple comparisons test. *Stance width*, $t_{(14)}$=3.329, p=0.005. *Stride length*, two-way ANOVA genotype $F_{(1,28)}$=3.164, p=0.086, limb $F_{(1,28)}$=0.02, p=0.887, interaction $F_{(1,28)}$=0.0001, p=0.989).

DOI: https://doi.org/10.7554/eLife.36691.010

The following video and figure supplements are available for figure 3:

Figure supplement 1. Representative examples of control and ChAT-CKO spinal cords demonstrate significant kyphotic curvature.

DOI: https://doi.org/10.7554/eLife.36691.011

Figure supplement 2. ChAT-CKO mice are significantly hypoactive.

DOI: https://doi.org/10.7554/eLife.36691.012

Figure 3—video 1. Representative video demonstrating tremulousness, kyphosis, and hyperactivity in ChAT-CKO mice, as compared to controls.

DOI: https://doi.org/10.7554/eLife.36691.013

Figure 3 continued on next page

Figure 3 continued

Figure 3—video 2. ChAT-CKO exhibit twisting and tremulousness, but not limb clasping during tail suspension.
DOI: https://doi.org/10.7554/eLife.36691.014

result in complex dystonia (***Jankovic and Patel, 1983***; ***LeDoux and Brady, 2003***; ***Loher and Krauss, 2009***; ***Zweig et al., 1988***; ***Mente et al., 2018***). Systematic cholinergic brainstem cell counts have not been performed in DYT1 dystonia postmortem samples; most studies have failed to demonstrate neuronal inclusions or overt cell loss in this region (***Paudel et al., 2014***; ***Pratt et al., 2016***; ***McNaught et al., 2004***).

Motor behavior is severely disrupted in ChAT-CKO mice, but is distinct from the Dlx-CKO phenotype (***Figure 3***; ***Table 1***). ChAT-CKO pups are initially indistinguishable from littermates, but at approximately 4 weeks of age develop a hunched posture, have unkempt fur, and exhibit reduced responsiveness to handling (***Figure 3A***, ***Figure 3—figure supplement 1***). Whereas normal mice exhibit a slight dorsal spinal curvature at rest, ChAT-CKO mice exhibit severe kyphosis, including during locomotion (assessed by two observers blind to experimental conditions; ***Figure 3B***; ***Figure 3—figure supplement 1***; ***Figure 3—video 1***) (***Guyenet et al., 2010***). ChAT-CKO mice also exhibit signs of weakness, including a significantly reduced ability to hang by the forelimbs (***Figure 3C***), tremulous movements, labored breathing (***Figure 3—video 1***), and significantly reduced horizontal and vertical movement in the open field (***Figure 3D,E***, ***Figure 3—figure supplement 2***). Remarkably, performance on the accelerating rotarod during two days of training appears normal (***Figure 3F***). The normal rotarod behavior differs from models of motor neuron and neuromuscular disease, suggesting that neuromuscular weakness is modest in ChAT-CKO, and less likely to contribute to other behavioral phenotypes (e.g., postural abnormality). The gait of ChAT-CKO mice is also significantly altered (***Figure 3G–I***). This constellation of behavioral phenotypes is distinct from Dlx-CKO mice (***Table 1***), in which loss of dorsal striatal ChI is associated with a set of persistent abnormal action-induced motor behaviors, including limb clasping and trunk twisting during tail suspension and open field hyperactivity (***Pappas et al., 2015***). ChAT-CKO mice did not exhibit fore- or hindlimb clasping during tail suspension, but did exhibit tremulousness and trunk twisting (15 CKO, 19 heterozygous, 22 Cre control, and 19 wild type mice observed; ***Figure 3—video 2***). These results suggest that dorsal striatal ChI neurodegeneration may not, by itself, be sufficient to cause limb clasping during tail suspension. However, the co-occurrence of brainstem and spinal cord

Table 1. Behavioral properties of Dlx-CKO and ChAT-CKO mice.

Motor function	Dlx-CKO	ChAT-CKO
	Pappas et al., 2015 eLife 4:e08352	present manuscript
Tail suspension	Trunk twisting	Trunk twisting
	Forelimb clasping	-
	Hindlimb clasping	-
	-	Tremulousness
Open field	Hyperactivity	Hypoactivity
Rotarod	Normal	Normal
Response to handling	Exaggerated	Reduced
Weakness, latency to fall	Grid hang reduction	Wire hang reduction
Gait	Normal by eye	Abnormal by eye
	Slightly reduced stance width	Increased stance width
	-	Increased paw angle
Overt postural abnormalities	-	Severe kyphosis
Tremulous movement	-	Severe
Labored breathing	-	Severe

DOI: https://doi.org/10.7554/eLife.36691.015

Table 2. Vulnerability of cholinergic populations.
(*)=Unconfirmed by independent marker.

	Cre expression		Cell death vulnerability	
Cholinergic population	**Dlx-Cre**	**ChAT-Cre**	**Dlx-Cre**	**ChAT-Cre**
Dorsolateral striatum (including dorsal caudate putamen)	Confirmed	Confirmed	Severe	Severe
Dorsomedial striatum (including ventral caudate putamen)	Confirmed	Confirmed	Mild	Spared
Nucleus accumbens	Confirmed	Confirmed	-	-
Basal forebrain	Confirmed	Confirmed	Spared	Spared
Cholinergic Brainstem	Absent	Confirmed	n/a	Severe (*)
Primary Motor Neurons	Absent	Confirmed	n/a	Moderate

DOI: https://doi.org/10.7554/eLife.36691.016

Table 3. Properties of cholinergic neuronal populations.
'Nucleus Basalis Complex'=Nucleus Basalis of Meynert, Horizontal limb of the diagonal band of Broca, Ventral Pallidum, Magnocellular Preoptic Area, Substantia Inominata, Nucleus of the Ansa Lenticularis. 'Septa"l = Medial Septum, Vertical Limb of the Diagonal Band of Broca. 'Cholinergic Brainstem'=Pedunculopontine Nucleus, Laterodorsal Tegmental Nucleus (***Pappas et al., 2015***; ***Mena-Segovia and Bolam, 2017***; ***Gonzales and Smith, 2015***; ***Manns et al., 2000***; ***Unal et al., 2012***; ***Petzold et al., 2015***; ***Kanning et al., 2010***; ***Kreitzer, 2009***; ***Zaborszky et al., 2012***; ***Garcia-Rill, 1991***; ***Semba et al., 1988***; ***Semba and Fibiger, 1992***; ***Phelps et al., 1990a***; ***Phelps et al., 1988***; ***Phelps et al., 1990b***; ***Phelps et al., 1989***; ***Aroca and Puelles, 2005***; ***Schambra et al., 1989***).

Cholinergic population	**Neuronal class**	**Firing properties**	**Efferent projections**	**Afferent inputs**	**Birth date/ final mitosis**	**Embryonic origin**	**ChAT expression**
Dorsolateral striatum (including dorsal caudate putamen)	Interneuron	tonically active, 2–10 Hz baseline firing rate	Local - striatal spiny projection neurons and fast spiking interneurons	Thalamus, sensorimotor cortex, striatal spiny projection neurons, striatal interneurons	E12-E15	MGE	~E16
Dorsomedial striatum (including ventral caudate putamen)	Interneuron	tonically active, 2–10 Hz baseline firing rate	Local - striatal spiny projection neurons and fast spiking interneurons	Thalamus, association cortices, striatal spiny projection neurons, striatal interneurons	E12-E15	MGE	~E16
Nucleus accumbens	Interneuron	tonically active, 0.6–12 Hz baseline firing rate	Local - striatal spiny projection neurons and fast spiking interneurons	Thalamus, frontal cortex, striatal spiny projection neurons, striatal interneurons	E12-E15	MGE	~E16
Basal forebrain	Projection neuron	Tonic/burst, subtype dependent	Cortex (Nucleus Basalis Complex), Hippocampus (Septal)	Medulla, locus ceruleus, substantia nigra, ventral tegmental area, hypothalamic nuclei, nucleus accumbens, amygdala, local intrinsic GABAergic and glutamatergic collaterals	E11-E15	POA/MGE	~E15-16
Cholinergic Brainstem	Projection neuron	episodic	Midbrain, superior colliculus, thalamus, globus pallidus, hypothalamus, septum, striatum, cortex	Brainstem reticular formation, midbrain central gray, lateral hypothalamus-zona incerta, cortex, amygdala, basal forebrain, basal ganglia output nuclei, brainstem and spinal cord sensory nuclei	E12-E13	Ventral rhombomere 1 (r1)	
Primary Motor Neurons	Projection neuron	subtype dependent	Muscle	Motor Cortex, local spinal cord interneurons and sensory neurons	E11-E12	Ventral spinal cord progenitor domains	E13

DOI: https://doi.org/10.7554/eLife.36691.017

neurodegeneration and tremulousness in ChAT-CKO mice could modify a clasping phenotype and therefore limit this strength of this conclusion.

While no single system or experimental approach can fully model a disease, the extreme postural abnormalities (kyphosis and twisting) in ChAT-CKO mice are reminiscent of Oppenheim's original description of dystonia (**Klein and Fahn, 2013**), suggesting that a constellation of cholinergic abnormalities may contribute to such a phenotype. The abnormal gait, tremulous movement, weakness, labored breathing, and appearance of reduced muscle mass in ChAT-CKO mice are consistent with brainstem and spinal cord pathology, yet the time course of ChAT-CKO abnormalities (beginning during development) differ from motor neuron and neuromuscular disease models, in which behavioral phenotypes typically emerge in adulthood (9–11 months of age; (**Dickinson and Meikle, 1973**; **Bridges et al., 1992**; **Deconinck et al., 1997**; **Grady et al., 1997**; **Laws and Hoey, 2004**; **Liu et al., 2016**; **Sopher et al., 2004**; **Monks et al., 2007**). Early motor behavioral manifestations also occur in Dlx-CKO and other DYT1 models, emphasizing the importance of torsinA function during development and maturation at behavioral (**Pappas et al., 2015**; **Liang et al., 2014**), cellular (**Pappas et al., 2018**), and molecular levels (**Tanabe et al., 2016**).

These findings establish a cell autonomous requirement of torsinA for the normal function and survival of distinct populations of cholinergic neurons. Comparison of basic cellular properties between susceptible and invulnerable cholinergic neuron populations does not identify obvious patterns driving selective vulnerability (**Tables 2** and **3**). Within the striatum, dorsal ChI are highly vulnerable to cell death, while ventral ChI are spared. It is unclear whether molecular differences within different ChI populations drive vulnerability, or if differences in connectivity or response to inputs contributes to their loss; these possibilities are not mutually exclusive. While often considered a single neuronal class, an existing and enlarging literature demonstrates that dorsal and ventral striatal ChI exhibit significant differences in morphology, regulation, and receptor expression (reviewed in [**Gonzales and Smith, 2015**]), as well as differing firing patterns during behavioral tasks (**Yarom and Cohen, 2011**) and responses to serotonergic input (**Virk et al., 2016**). These differences implicate the presence of multiple ChI subclasses, though it is important to note that the spared 'ventral' population here represents the ventral part of the dorsal striatum, not the nucleus accumbens. Thalamostriatal and corticostriatal input is highly topographic (**Alexander et al., 1986**; **Smith et al., 2004**), raising the possibility that aberrant input from different thalamic nuclei or cortical regions (or aberrant response to that input) could alter the susceptibility of dorsal vs ventral ChI. It is likely that a combination of these and other factors plays a role in the differential susceptibility of cholinergic neuronal populations, including their molecular profiles (e.g., protective factors in some neurons, susceptibility factors in others), the response to afferent inputs, and their inherent physiological properties.

These studies greatly strengthen the connection between torsinA and cholinergic dysfunction, demonstrating that specific cholinergic populations exhibit a cell autonomous selective vulnerability to torsinA deficiency, while others – basal forebrain and ventral striatum – are spared. These findings open novel avenues of study aimed at defining the molecular mechanisms responsible for this cell autonomous selective vulnerability, and circuit-level analyses to ameliorate the effects of cholinergic neurotransmission abnormalities.

Materials and methods

Key resources table

Reagent type (species) or resource	Designation	Source or reference	Identifiers	Additional information
Gene (Mus musculus)	*Tor1a*	NA	NCBI Gene: 30931; MGI:1353568	Encodes TorsinA
Strain, strain background(M. musculus)	ChAT-Cre	Jackson Laboratories	Stock ID 006410	$Chat^{tm2(cre)Lowl}$; (Chat-IRES-Cre)
Strain, strain background(M. musculus)	$Tor1a^{Flx/Flx}$	Jackson Laboratories	Stock ID 025832	$Tor1a^{tm3.1Wtd}$

Continued on next page

Continued

Reagent type (species) or resource	Designation	Source or reference	Identifiers	Additional information
Strain, strain background(M. musculus)	Tor1a$^{-/-}$	Jackson Laboratories	Stock ID 006251	Tor1a^{tm1Wtd}
Antibody	Choline Acetyltransferase	Millipore AB144P	RRID: AB_2079751	1:100
Antibody	P75 Neurotrophin Receptor	Santa Cruz sc6188	RRID: AB_2267254	1:100
Antibody	NeuN	Cell Signaling #12943	RRID: AB_2630395	1:500
Antibody	GFAP	Cell Signaling #3670P	RRID: AB_561049	1:1000
Antibody	Iba-1	Wako 019–19741	RRID: AB_839504	1:500
Antibody	TorsinA	Abcam ab34540	RRID: AB_2240792	1:100
Antibody	anti-mouse	ThermoFisher A-31571	RRID: AB_162542	1:800
Antibody	anti-rabbit	ThermoFisher A-21206	RRID: AB_2535792	1:800
Antibody	anti-rabbit	ThermoFisher A-31572	RRID: AB_162543	1:800
Antibody	anti-goat	ThermoFisher A-21432	RRID: AB_2535853	1:800
Antibody	anti-goat	Jackson Immunoresearch 705-065-003	RRID: AB_2340396	1:800
Commercial assay or kit	ABC HRP Kit (Standard)	Vector Laboratories	Pk-6100	Vectastain elite ABC kit

Animals

ChAT-CKO mice were generated by crossing *Chat*$^{tm2(cre)Lowl}$ mice (**Rossi et al., 2011**) with *Tor1a*$^{Flx/Flx}$ mice (**Liang et al., 2014**), using the breeding strategy described in (**Pappas et al., 2015**), and maintained as previously described (**Pappas et al., 2015**).

Sample size estimation

Sample sizes for histological and behavioral studies were determined by performing a power analysis of the open field or striatal cholinergic stereological data (mean and std. dev.) from (**Pappas et al., 2015**), an alpha of 0.01, and beta of 0.1. (Kane SP. Sample Size Calculator. ClinCalc: *http://clincalc.com/stats/samplesize.aspx*). Experimental cohorts were generated accordingly.

Table 4. Antibodies used for immunohistochemistry.

Level	Antigen	Host	Conjugated	Dilution	Source
Primary	Choline Acetyltransferase	Goat	-	1:100	Millipore AB144P
Primary	P75 Neurotrophin Receptor	Goat	-	1:100	Santa Cruz sc6188
Primary	NeuN	Rabbit	-	1:500	Cell Signaling #12943
Primary	GFAP	Mouse	-	1:1000	Cell Signaling #3670P
Primary	Iba-1	Rabbit	-	1:500	Wako 019–19741
Primary	TorsinA	Rabbit	-	1:100	Abcam ab34540
Secondary	anti-mouse	Donkey	Alexafluor-647	1:800	ThermoFisher A-31571
Secondary	anti-rabbit	Donkey	Alexafluor-488	1:800	ThermoFisher A-21206
Secondary	anti-rabbit	Donkey	Alexafluor-555	1:800	ThermoFisher A-31572
Secondary	anti-goat	Donkey	Alexafluor-555	1:800	ThermoFisher A-21432
Secondary	anti-goat	Donkey	biotin	1:800	Jackson Immunoresearch 705-065-003

DOI: https://doi.org/10.7554/eLife.36691.018

Table 5. Stereology parameters.

Region	Marker	Counting frame (μm)	Grid size (μm)	Guard zone (μm)	Dissector (μm)	Section cut thickness (μm)
Striatum	ChAT	100 × 100	250 × 250	1	10	40
NBM	P75	90 × 90	200 × 200	5	30	50
MS/VDB	P75	90 × 90	200 × 200	5	30	50
GP	P75	100 × 100	140 × 140	5	30	50
PPN and LDT	ChAT	75 × 75	150 × 150	5	30	50
PPN and LDT	NeuN	40 × 40	250 × 250	5	30	50

DOI: https://doi.org/10.7554/eLife.36691.019

Imaging and stereology

Brain sections were generated and stained with immunohistochemistry using the methods described in (***Pappas et al., 2015***; ***Pappas et al., 2018***). Antibodies and reagents are listed in ***Table 4***. Sections were observed with epifluorescence or brightfield microscopy (***Pappas et al., 2018***), and unbiased stereological cell counting was performed with StereoInvestigator software using the Optical Fractionator probe (specific parameters in ***Table 5***). Striatal cell density was quantified as done previously (***Pappas et al., 2015***). Spinal cord neurons were quantified as described in (***Kim et al., 2017***).

Behavioral analysis

Tail suspension, forelimb wire suspension, open field, accelerating rotarod, and gait analysis were performed as described in (***Pappas et al., 2015***). Kyphosis severity was scored as described in (***Guyenet et al., 2010***).

Statistical analysis

t-tests, one-way, or two-way ANOVA with posthoc corrections for multiple comparisons were performed to compare experimental groups (details in each figure legend). If variances were significantly different between groups, non-parametric tests were performed.

Acknowledgements

We thank Stephanie Mrowczynski for expert technical assistance and the Dauer lab for helpful comments and suggestions. This research was supported by generous support from Tyler's Hope for a Dystonia Cure and the following grants: RO1NS077730 (William T Dauer), RO1NS057482, R21NS099921, and R56NS104218 (Umrao R Monani).

Additional information

Funding

Funder	Grant reference number	Author
National Institute of Neurological Disorders and Stroke	RO1NS077730	William T Dauer
Tyler's Hope for a Dystonia Cure		William T Dauer
National Institutes of Health	RO1NS057482	Umrao R Monani
National Institutes of Health	R21NS099921	Umrao R Monani
National Institutes of Health	R56NS104218	Umrao R Monani

The funders had no role in study design, data collection and interpretation, or the decision to submit the work for publication.

Author contributions

Samuel S Pappas, Conceptualization, Data curation, Formal analysis, Investigation, Writing—original draft, Writing—review and editing; Jay Li, Tessa M LeWitt, Formal analysis, Investigation, Writing—review and editing; Jeong-Ki Kim, Investigation, Writing—review and editing; Umrao R Monani, Resources, Supervision, Funding acquisition, Writing—review and editing; William T Dauer, Conceptualization, Resources, Supervision, Funding acquisition, Writing—review and editing

Author ORCIDs

Samuel S Pappas http://orcid.org/0000-0002-6980-2058
Jay Li http://orcid.org/0000-0002-8146-4450
Jeong-Ki Kim http://orcid.org/0000-0003-0218-1215
William T Dauer http://orcid.org/0000-0003-1775-7504

Ethics

Animal experimentation: All experiments were performed according to the recommendations in the Guide for the Care and Use of Laboratory Animals of the National Institutes of Health. All procedures involving animals were approved by the University of Michigan Institutional Animal Care and Use Committee (animal use protocol PRO00006600). All effort was taken to minimize the number of animals used and to prevent discomfort or distress.

Decision letter and Author response

Decision letter https://doi.org/10.7554/eLife.36691.023
Author response https://doi.org/10.7554/eLife.36691.024

Additional files

Supplementary files

- Transparent reporting form

DOI: https://doi.org/10.7554/eLife.36691.020

Data availability

All data generated during this study are included in the manuscript and supporting files

References

Albin RL, Cross D, Cornblath WT, Wald JA, Wernette K, Frey KA, Minoshima S. 2003. Diminished striatal [123I] iodobenzovesamicol binding in idiopathic cervical dystonia. *Annals of Neurology* **53**:528–532. DOI: https://doi.org/10.1002/ana.10527, PMID: 12666122

Alexander GE, DeLong MR, Strick PL. 1986. Parallel organization of functionally segregated circuits linking basal ganglia and cortex. *Annual Review of Neuroscience* **9**:357–381. DOI: https://doi.org/10.1146/annurev.ne.09.030186.002041, PMID: 3085570

Aroca P, Puelles L. 2005. Postulated boundaries and differential fate in the developing rostral hindbrain. *Brain Research Reviews* **49**:179–190. DOI: https://doi.org/10.1016/j.brainresrev.2004.12.031, PMID: 16111548

Ballinger EC, Ananth M, Talmage DA, Role LW. 2016. Basal Forebrain Cholinergic Circuits and Signaling in Cognition and Cognitive Decline. *Neuron* **91**:1199–1218. DOI: https://doi.org/10.1016/j.neuron.2016.09.006, PMID: 27657448

Blanco-Lezcano L, Jimenez-Martin J, Díaz-Hung ML, Alberti-Amador E, Wong-Guerra M, González-Fraguela ME, Estupiñán-Díaz B, Serrano-Sánchez T, Francis-Turner L, Delgado-Ocaña S, Núñez-Figueredo Y, Vega-Hurtado Y, Fernández-Jiménez I. 2017. Motor dysfunction and alterations in glutathione concentration, cholinesterase activity, and BDNF expression in substantia nigra pars compacta in rats with pedunculopontine lesion. *Neuroscience* **348**:83–97. DOI: https://doi.org/10.1016/j.neuroscience.2017.02.008, PMID: 28212832

Bohnen NI, Müller ML, Koeppe RA, Studenski SA, Kilbourn MA, Frey KA, Albin RL. 2009. History of falls in Parkinson disease is associated with reduced cholinergic activity. *Neurology* **73**:1670–1676. DOI: https://doi.org/10.1212/WNL.0b013e3181c1ded6, PMID: 19917989

Bridges LR, Coulton GR, Howard G, Moss J, Mason RM. 1992. The neuromuscular basis of hereditary kyphoscoliosis in the mouse. *Muscle & Nerve* **15**:172–179. DOI: https://doi.org/10.1002/mus.880150208, PMID: 1372391

Burke RE, Fahn S, Marsden CD. 1986. Torsion dystonia: a double-blind, prospective trial of high-dosage trihexyphenidyl. *Neurology* **36**:160–164. DOI: https://doi.org/10.1212/WNL.36.2.160, PMID: 3511401

Capelli P, Pivetta C, Soledad Esposito M, Arber S. 2017. Locomotor speed control circuits in the caudal brainstem. *Nature* **551**:373–377. DOI: https://doi.org/10.1038/nature24064, PMID: 29059682

Dautan D, Huerta-Ocampo I, Witten IB, Deisseroth K, Bolam JP, Gerdjikov T, Mena-Segovia J. 2014. A major external source of cholinergic innervation of the striatum and nucleus accumbens originates in the brainstem. *Journal of Neuroscience* **34**:4509–4518. DOI: https://doi.org/10.1523/JNEUROSCI.5071-13.2014, PMID: 24671996

Deconinck AE, Rafael JA, Skinner JA, Brown SC, Potter AC, Metzinger L, Watt DJ, Dickson JG, Tinsley JM, Davies KE. 1997. Utrophin-dystrophin-deficient mice as a model for Duchenne muscular dystrophy. *Cell* **90**:717–727. DOI: https://doi.org/10.1016/S0092-8674(00)80532-2, PMID: 9288751

Dickinson AG, Meikle VM. 1973. Genetic kyphoscoliosis in mice. *The Lancet* **1**:1186. DOI: https://doi.org/10.1016/S0140-6736(73)91186-0, PMID: 4123573

Eskow Jaunarajs KL, Bonsi P, Chesselet MF, Standaert DG, Pisani A. 2015. Striatal cholinergic dysfunction as a unifying theme in the pathophysiology of dystonia. *Progress in Neurobiology* **127-128**:91–107. DOI: https://doi.org/10.1016/j.pneurobio.2015.02.002, PMID: 25697043

Garcia-Rill E. 1991. The pedunculopontine nucleus. *Progress in Neurobiology* **36**:363–389. DOI: https://doi.org/10.1016/0301-0082(91)90016-T, PMID: 1887068

Gonzales KK, Smith Y. 2015. Cholinergic interneurons in the dorsal and ventral striatum: anatomical and functional considerations in normal and diseased conditions. *Annals of the New York Academy of Sciences* **1349**:1–45. DOI: https://doi.org/10.1111/nyas.12762, PMID: 25876458

Grabli D, Karachi C, Folgoas E, Monfort M, Tande D, Clark S, Civelli O, Hirsch EC, François C. 2013. Gait disorders in parkinsonian monkeys with pedunculopontine nucleus lesions: a tale of two systems. *Journal of Neuroscience* **33**:11986–11993. DOI: https://doi.org/10.1523/JNEUROSCI.1568-13.2013, PMID: 23864685

Grady RM, Teng H, Nichol MC, Cunningham JC, Wilkinson RS, Sanes JR. 1997. Skeletal and cardiac myopathies in mice lacking utrophin and dystrophin: a model for Duchenne muscular dystrophy. *Cell* **90**:729–738. DOI: https://doi.org/10.1016/S0092-8674(00)80533-4, PMID: 9288752

Guyenet SJ, Furrer SA, Damian VM, Baughan TD, La Spada AR, Garden GA. 2010. A simple composite phenotype scoring system for evaluating mouse models of cerebellar ataxia. *Journal of Visualized Experiments*. DOI: https://doi.org/10.3791/1787, PMID: 20495529

Haber SN. 2016. Corticostriatal circuitry. *Dialogues in Clinical Neuroscience* **18**:7–21. PMID: 27069376

Hasselmo ME, Sarter M. 2011. Modes and models of forebrain cholinergic neuromodulation of cognition. *Neuropsychopharmacology* **36**:52–73. DOI: https://doi.org/10.1038/npp.2010.104, PMID: 20668433

Jankovic J, Patel SC. 1983. Blepharospasm associated with brainstem lesions. *Neurology* **33**:1237–1240. DOI: https://doi.org/10.1212/WNL.33.9.1237, PMID: 6684264

Kaneko S, Hikida T, Watanabe D, Ichinose H, Nagatsu T, Kreitman RJ, Pastan I, Nakanishi S. 2000. Synaptic integration mediated by striatal cholinergic interneurons in basal ganglia function. *Science* **289**:633–637. DOI: https://doi.org/10.1126/science.289.5479.633, PMID: 10915629

Kanning KC, Kaplan A, Henderson CE. 2010. Motor neuron diversity in development and disease. *Annual Review of Neuroscience* **33**:409–440. DOI: https://doi.org/10.1146/annurev.neuro.051508.135722, PMID: 20367447

Karachi C, Grabli D, Bernard FA, Tandé D, Wattiez N, Belaid H, Bardinet E, Prigent A, Nothacker HP, Hunot S, Hartmann A, Lehéricy S, Hirsch EC, François C. 2010. Cholinergic mesencephalic neurons are involved in gait and postural disorders in Parkinson disease. *Journal of Clinical Investigation* **120**:2745–2754. DOI: https://doi.org/10.1172/JCI42642, PMID: 20628197

Kim JK, Caine C, Awano T, Herbst R, Monani UR. 2017. Motor neuronal repletion of the NMJ organizer, Agrin, modulates the severity of the spinal muscular atrophy disease phenotype in model mice. *Human Molecular Genetics* **26**:2377–2385. DOI: https://doi.org/10.1093/hmg/ddx124, PMID: 28379354

Klein C, Fahn S. 2013. Translation of Oppenheim's 1911 paper on dystonia. *Movement Disorders* **28**:851–862. DOI: https://doi.org/10.1002/mds.25546, PMID: 23893442

Kreitzer AC. 2009. Physiology and pharmacology of striatal neurons. *Annual Review of Neuroscience* **32**:127–147. DOI: https://doi.org/10.1146/annurev.neuro.051508.135422, PMID: 19400717

Laws N, Hoey A. 2004. Progression of kyphosis in mdx mice. *Journal of Applied Physiology*. **97**:1970–1977. DOI: https://doi.org/10.1152/japplphysiol.01357.2003, PMID: 15234960

LeDoux MS, Brady KA. 2003. Secondary cervical dystonia associated with structural lesions of the central nervous system. *Movement Disorders* **18**:60–69. DOI: https://doi.org/10.1002/mds.10301, PMID: 12518301

Liang CC, Tanabe LM, Jou S, Chi F, Dauer WT. 2014. TorsinA hypofunction causes abnormal twisting movements and sensorimotor circuit neurodegeneration. *Journal of Clinical Investigation* **124**:3080–3092. DOI: https://doi.org/10.1172/JCI72830, PMID: 24937429

Liu Y, Pattamatta A, Zu T, Reid T, Bardhi O, Borchelt DR, Yachnis AT, Ranum LP. 2016. C9orf72 BAC Mouse Model with Motor Deficits and Neurodegenerative Features of ALS/FTD. *Neuron* **90**:521–534. DOI: https://doi.org/10.1016/j.neuron.2016.04.005, PMID: 27112499

Loher TJ, Krauss JK. 2009. Dystonia associated with pontomesencephalic lesions. *Movement Disorders* **24**:157–167. DOI: https://doi.org/10.1002/mds.22196, PMID: 18951533

MacLaren DA, Markovic T, Clark SD. 2014a. Assessment of sensorimotor gating following selective lesions of cholinergic pedunculopontine neurons. *European Journal of Neuroscience* **40**:3526–3537. DOI: https://doi.org/10.1111/ejn.12716, PMID: 25208852

MacLaren DA, Santini JA, Russell AL, Markovic T, Clark SD. 2014b. Deficits in motor performance after pedunculopontine lesions in rats–impairment depends on demands of task. *European Journal of Neuroscience* **40**:3224–3236. DOI: https://doi.org/10.1111/ejn.12666, PMID: 24995993

Madisen L, Zwingman TA, Sunkin SM, Oh SW, Zariwala HA, Gu H, Ng LL, Palmiter RD, Hawrylycz MJ, Jones AR, Lein ES, Zeng H. 2010. A robust and high-throughput Cre reporting and characterization system for the whole mouse brain. *Nature Neuroscience* **13**:133–140. DOI: https://doi.org/10.1038/nn.2467, PMID: 20023653

Maltese M, Martella G, Madeo G, Fagiolo I, Tassone A, Ponterio G, Sciamanna G, Burbaud P, Conn PJ, Bonsi P, Pisani A. 2014. Anticholinergic drugs rescue synaptic plasticity in DYT1 dystonia: role of M1 muscarinic receptors. *Movement Disorders* **29**:1655–1665. DOI: https://doi.org/10.1002/mds.26009, PMID: 25195914

Manns ID, Alonso A, Jones BE. 2000. Discharge properties of juxtacellularly labeled and immunohistochemically identified cholinergic basal forebrain neurons recorded in association with the electroencephalogram in anesthetized rats. *The Journal of Neuroscience* **20**:1505–1518. DOI: https://doi.org/10.1523/JNEUROSCI.20-04-01505.2000, PMID: 10662840

Martella G, Tassone A, Sciamanna G, Platania P, Cuomo D, Viscomi MT, Bonsi P, Cacci E, Biagioni S, Usiello A, Bernardi G, Sharma N, Standaert DG, Pisani A. 2009. Impairment of bidirectional synaptic plasticity in the striatum of a mouse model of DYT1 dystonia: role of endogenous acetylcholine. *Brain* **132**:2336–2349. DOI: https://doi.org/10.1093/brain/awp194, PMID: 19641103

McNaught KS, Kapustin A, Jackson T, Jengelley TA, Jnobaptiste R, Shashidharan P, Perl DP, Pasik P, Olanow CW. 2004. Brainstem pathology in DYT1 primary torsion dystonia. *Annals of Neurology* **56**:540–547. DOI: https://doi.org/10.1002/ana.20225, PMID: 15455404

Mena-Segovia J, Bolam JP. 2017. Rethinking the Pedunculopontine Nucleus: From Cellular Organization to Function. *Neuron* **94**:7–18. DOI: https://doi.org/10.1016/j.neuron.2017.02.027, PMID: 28384477

Mena-Segovia J, Micklem BR, Nair-Roberts RG, Ungless MA, Bolam JP. 2009. GABAergic neuron distribution in the pedunculopontine nucleus defines functional subterritories. *The Journal of Comparative Neurology* **515**:397–408. DOI: https://doi.org/10.1002/cne.22065, PMID: 19459217

Mena-Segovia J. 2016. Structural and functional considerations of the cholinergic brainstem. *Journal of Neural Transmission* **123**:731–736. DOI: https://doi.org/10.1007/s00702-016-1530-9, PMID: 26945862

Mente K, Edwards NA, Urbano D, Ray-Chaudhury A, Iacono D, Alho A, Alho EJL, Amaro E, Horovitz SG, Hallett M. 2018. Pedunculopontine Nucleus Cholinergic Deficiency in Cervical Dystonia. *Movement Disorders* **33**:827–834. DOI: https://doi.org/10.1002/mds.27358, PMID: 29508906

Monks DA, Johansen JA, Mo K, Rao P, Eagleson B, Yu Z, Lieberman AP, Breedlove SM, Jordan CL. 2007. Overexpression of wild-type androgen receptor in muscle recapitulates polyglutamine disease. *PNAS* **104**:18259–18264. DOI: https://doi.org/10.1073/pnas.0705501104, PMID: 17984063

Ozelius LJ, Hewett JW, Page CE, Bressman SB, Kramer PL, Shalish C, de Leon D, Brin MF, Raymond D, Corey DP, Fahn S, Risch NJ, Buckler AJ, Gusella JF, Breakefield XO. 1997. The early-onset torsion dystonia gene (DYT1) encodes an ATP-binding protein. *Nature Genetics* **17**:40–48. DOI: https://doi.org/10.1038/ng0997-40, PMID: 9288096

Pappas SS, Darr K, Holley SM, Cepeda C, Mabrouk OS, Wong JM, LeWitt TM, Paudel R, Houlden H, Kennedy RT, Levine MS, Dauer WT. 2015. Forebrain deletion of the dystonia protein torsinA causes dystonic-like movements and loss of striatal cholinergic neurons. *eLife* **4**:e08352. DOI: https://doi.org/10.7554/eLife.08352, PMID: 26052670

Pappas SS, Leventhal DK, Albin RL, Dauer WT. 2014. Mouse models of neurodevelopmental disease of the basal ganglia and associated circuits. *Current Topics in Developmental Biology* **109**:97–169. DOI: https://doi.org/10.1016/B978-0-12-397920-9.00001-9, PMID: 24947237

Pappas SS, Liang CC, Kim S, Rivera CO, Dauer WT. 2018. TorsinA dysfunction causes persistent neuronal nuclear pore defects. *Human Molecular Genetics* **27**:407–420. DOI: https://doi.org/10.1093/hmg/ddx405, PMID: 29186574

Parent A, Hazrati LN. 1995. Functional anatomy of the basal ganglia. I. The cortico-basal ganglia-thalamo-cortical loop. *Brain Research Reviews* **20**:91–127. DOI: https://doi.org/10.1016/0165-0173(94)00007-C, PMID: 7711769

Paudel R, Kiely A, Li A, Lashley T, Bandopadhyay R, Hardy J, Jinnah HA, Bhatia K, Houlden H, Holton JL. 2014. Neuropathological features of genetically confirmed DYT1 dystonia: investigating disease-specific inclusions. *Acta Neuropathologica Communications* **2**:159. DOI: https://doi.org/10.1186/s40478-014-0159-x, PMID: 25403864

Petzold A, Valencia M, Pál B, Mena-Segovia J. 2015. Decoding brain state transitions in the pedunculopontine nucleus: cooperative phasic and tonic mechanisms. *Frontiers in Neural Circuits* **9**:68. DOI: https://doi.org/10.3389/fncir.2015.00068, PMID: 26582977

Phelps PE, Barber RP, Brennan LA, Maines VM, Salvaterra PM, Vaughn JE. 1990a. Embryonic development of four different subsets of cholinergic neurons in rat cervical spinal cord. *The Journal of Comparative Neurology* **291**:9–26. DOI: https://doi.org/10.1002/cne.902910103, PMID: 2298930

Phelps PE, Barber RP, Vaughn JE. 1988. Generation patterns of four groups of cholinergic neurons in rat cervical spinal cord: a combined tritiated thymidine autoradiographic and choline acetyltransferase immunocytochemical study. *The Journal of Comparative Neurology* **273**:459–472. DOI: https://doi.org/10.1002/cne.902730403, PMID: 3209733

Phelps PE, Brady DR, Vaughn JE. 1989. The generation and differentiation of cholinergic neurons in rat caudate-putamen. *Developmental Brain Research* **46**:47–60. DOI: https://doi.org/10.1016/0165-3806(89)90142-9, PMID: 2706771

Phelps PE, Brennan LA, Vaughn JE. 1990b. Generation patterns of immunocytochemically identified cholinergic neurons in rat brainstem. *Developmental Brain Research* **56**:63–74. DOI: https://doi.org/10.1016/0165-3806(90)90165-U, PMID: 2279332

Pisani A, Martella G, Tscherter A, Bonsi P, Sharma N, Bernardi G, Standaert DG. 2006. Altered responses to dopaminergic D2 receptor activation and N-type calcium currents in striatal cholinergic interneurons in a mouse model of DYT1 dystonia. *Neurobiology of Disease* **24**:318–325. DOI: https://doi.org/10.1016/j.nbd.2006.07.006, PMID: 16934985

Pratt D, Mente K, Rahimpour S, Edwards NA, Tinaz S, Berman BD, Hallett M, Ray-Chaudhury A. 2016. Diminishing evidence for torsinA-positive neuronal inclusions in DYT1 dystonia. *Acta Neuropathologica Communications* **4**:85. DOI: https://doi.org/10.1186/s40478-016-0362-z, PMID: 27531128

Roseberry TK, Lee AM, Lalive AL, Wilbrecht L, Bonci A, Kreitzer AC. 2016. Cell-Type-Specific Control of Brainstem Locomotor Circuits by Basal Ganglia. *Cell* **164**:526–537. DOI: https://doi.org/10.1016/j.cell.2015.12.037, PMID: 26824660

Rossi J, Balthasar N, Olson D, Scott M, Berglund E, Lee CE, Choi MJ, Lauzon D, Lowell BB, Elmquist JK. 2011. Melanocortin-4 receptors expressed by cholinergic neurons regulate energy balance and glucose homeostasis. *Cell Metabolism* **13**:195–204. DOI: https://doi.org/10.1016/j.cmet.2011.01.010, PMID: 21284986

Schambra UB, Sulik KK, Petrusz P, Lauder JM. 1989. Ontogeny of cholinergic neurons in the mouse forebrain. *The Journal of Comparative Neurology* **288**:101–122. DOI: https://doi.org/10.1002/cne.902880109, PMID: 2794134

Sciamanna G, Hollis R, Ball C, Martella G, Tassone A, Marshall A, Parsons D, Li X, Yokoi F, Zhang L, Li Y, Pisani A, Standaert DG. 2012b. Cholinergic dysregulation produced by selective inactivation of the dystonia-associated protein torsinA. *Neurobiology of Disease* **47**:416–427. DOI: https://doi.org/10.1016/j.nbd.2012.04.015, PMID: 22579992

Sciamanna G, Tassone A, Mandolesi G, Puglisi F, Ponterio G, Martella G, Madeo G, Bernardi G, Standaert DG, Bonsi P, Pisani A. 2012a. Cholinergic dysfunction alters synaptic integration between thalamostriatal and corticostriatal inputs in DYT1 dystonia. *Journal of Neuroscience* **32**:11991–12004. DOI: https://doi.org/10.1523/JNEUROSCI.0041-12.2012, PMID: 22933784

Semba K, Fibiger HC. 1992. Afferent connections of the laterodorsal and the pedunculopontine tegmental nuclei in the rat: a retro- and antero-grade transport and immunohistochemical study. *The Journal of Comparative Neurology* **323**:387–410. DOI: https://doi.org/10.1002/cne.903230307, PMID: 1281170

Semba K, Vincent SR, Fibiger HC. 1988. Different times of origin of choline acetyltransferase- and somatostatin-immunoreactive neurons in the rat striatum. *The Journal of Neuroscience* **8**:3937–3944. DOI: https://doi.org/10.1523/JNEUROSCI.08-10-03937.1988, PMID: 2903916

Smith Y, Raju DV, Pare JF, Sidibe M. 2004. The thalamostriatal system: a highly specific network of the basal ganglia circuitry. *Trends in Neurosciences* **27**:520–527. DOI: https://doi.org/10.1016/j.tins.2004.07.004, PMID: 15331233

Sopher BL, Thomas PS, LaFevre-Bernt MA, Holm IE, Wilke SA, Ware CB, Jin LW, Libby RT, Ellerby LM, La Spada AR. 2004. Androgen receptor YAC transgenic mice recapitulate SBMA motor neuronopathy and implicate VEGF164 in the motor neuron degeneration. *Neuron* **41**:687–699. DOI: https://doi.org/10.1016/S0896-6273(04)00082-0, PMID: 15003169

Syed A, Baker PM, Ragozzino ME. 2016. Pedunculopontine tegmental nucleus lesions impair probabilistic reversal learning by reducing sensitivity to positive reward feedback. *Neurobiology of Learning and Memory* **131**:1–8. DOI: https://doi.org/10.1016/j.nlm.2016.03.010, PMID: 26976089

Tanabe LM, Liang CC, Dauer WT. 2016. Neuronal Nuclear Membrane Budding Occurs during a Developmental Window Modulated by Torsin Paralogs. *Cell Reports* **16**:3322–3333. DOI: https://doi.org/10.1016/j.celrep.2016.08.044, PMID: 27653693

Unal CT, Golowasch JP, Zaborszky L. 2012. Adult mouse basal forebrain harbors two distinct cholinergic populations defined by their electrophysiology. *Frontiers in Behavioral Neuroscience* **6**:21. DOI: https://doi.org/10.3389/fnbeh.2012.00021, PMID: 22586380

Virk MS, Sagi Y, Medrihan L, Leung J, Kaplitt MG, Greengard P. 2016. Opposing roles for serotonin in cholinergic neurons of the ventral and dorsal striatum. *Proceedings of the National Academy of Sciences* **113**:734–739. DOI: https://doi.org/10.1073/pnas.1524183113, PMID: 26733685

Wang HL, Morales M. 2009. Pedunculopontine and laterodorsal tegmental nuclei contain distinct populations of cholinergic, glutamatergic and GABAergic neurons in the rat. *European Journal of Neuroscience* **29**:340–358. DOI: https://doi.org/10.1111/j.1460-9568.2008.06576.x, PMID: 19200238

Xiao C, Cho JR, Zhou C, Treweek JB, Chan K, McKinney SL, Yang B, Gradinaru V. 2016. Cholinergic Mesopontine Signals Govern Locomotion and Reward through Dissociable Midbrain Pathways. *Neuron* **90**:333–347. DOI: https://doi.org/10.1016/j.neuron.2016.03.028, PMID: 27100197

Yarom O, Cohen D. 2011. Putative cholinergic interneurons in the ventral and dorsal regions of the striatum have distinct roles in a two choice alternative association task. *Frontiers in Systems Neuroscience* **5**:36. DOI: https://doi.org/10.3389/fnsys.2011.00036, PMID: 21660109

Zaborszky L, van den Pol A, Gyengesi E. 2012. The basal forebrain cholinergic projection system in mice. In: *The Mouse Nervous System*. p. 684–714 . DOI: https://doi.org/10.1016/B978-0-12-369497-3.10028-7

Zweig RM, Hedreen JC, Jankel WR, Casanova MF, Whitehouse PJ, Price DL. 1988. Pathology in brainstem regions of individuals with primary dystonia. *Neurology* **38**:702–706. DOI: https://doi.org/10.1212/WNL.38.5.702, PMID: 3362365